Experimental Parasitology 248 (2023) 108498

Contents lists available at ScienceDirect

Experimental Parasitology

journal homepage: www.elsevier.com/locate/yexpr

Synthesis, characterization, antioxidant and antiparasitic activities new naphthyl-thiazole derivatives

Natali de França Nibbering Santos [a], Natanael da Silva Bezerra Junior [a], Jamerson Ferreira de Oliveira [b], Denise Maria Figueiredo Araújo Duarte [c], José Cleberson dos Santos Soares [a], Diego Santa Clara Marques [a], Aline Caroline da Silva Santos [d], Fátima Nogueira [c], Valéria Rêgo Alves Pereira [d], Maria Carmo Alves de Lima [a], Iranildo José da Cruz Filho [a,*]

[a] *Federal University of Pernambuco (UFPE), Department of Antibiotics, 50670-901, Recife, PE, Brazil*
[b] *University of International Integration of Afro-Brazilian Lusophony (UNILAB), 62790-970, Redenção, CE, Brazil*
[c] *Global Health and Tropical Medicine, Institute of Hygiene and Tropical Medicine, Universidade Nova de Lisboa, 1349-008, Lisbon, Portugal*
[d] *Oswaldo Cruz Pernambuco Foundation (Fiocruz/PE), Department of Immunology, 50670-420, Recife, PE, Brazil*

ARTICLE INFO

Keywords:
Thiosemicarbazones
Thiazoles
Cytotoxicity in animal cells
Leishmania
Trypanosoma cruzi
Plasmodium falciparum

ABSTRACT

In this work, 13 thiosemicarbazones (1a – m) and 16 thiazoles (2a – p) were obtained, which were properly characterized by spectroscopic and spectrometric techniques. The pharmacokinetic properties obtained *in silico* revealed that the derivatives are in accordance with the parameters established by lipinski and veber, showing that such compounds have good bioavailability or permeability when administered orally. In assays of antioxidant activity, thiosemicarbazones showed moderate to high antioxidant potential when compared to thiazoles. In addition, they were able to interact with albumin and DNA. Screening assays to assess the toxicity of compounds to mammalian cells revealed that thiosemicarbazones were less toxic when compared to thiazoles. In relation to *in vitro* antiparasitic activity, thiosemicarbazones and thiazoles showed cytotoxic potential against the parasites *Leishmania amazonensis* and *Trypanosoma cruzi*. Among the compounds, 1b, 1j and 2l stood out, showing inhibition potential for the amastigote forms of the two parasites. As for the *in vitro* antimalarial activity, thiosemicarbazones did not inhibit *Plasmodium falciparum* growth. In contrast, thiazoles promoted growth inhibition. This study shows in a preliminary way that the synthesized compounds have antiparasitic potential *in vitro*.

1. Introduction

Neglected tropical diseases (NTDs) refer to a group of global health problems caused mainly by parasitic organisms affecting a population with low socioeconomic status, causing high rates of morbidity and mortality. According to the World Health Organization (WHO), 17 diseases are part of this group, affecting about 1 billion people in the world, with 70% of the affected territories being low- and middle-income economies (Ramsay et al., 2016; World Health Organization, 2018; Ruiz-Postigo et al. 2021; World Health Organization, 2022).

In this context, some parasitoses caused by *Leishmania* species, *Trypanosoma cruzi* (*T. cruzi*), *Schistosoma mansoni*, *Plasmodium falciparum*, among others are included. Epidemiological data show that cases of NTDs have become a serious public health problem. Leishmaniasis has a wide range of clinical symptoms. According to the WHO it is estimated that 12 million people are affected by cutaneous or visceral leishmaniasis, and about 2 million infections occur each year. Approximately 350 million people are at risk in 88 countries around the world (Ruiz-Postigo et al. 2021; Santos Silva et al., 2021).

Chagas disease in recent decades has been detected in several countries outside Latin America, including the United States of America and Canada, European countries and some African, Eastern Mediterranean and Western Pacific countries. An estimated 6 to 7 million people have been infected with *T. cruzi* worldwide, with about 10,000 deaths year (World Health Organization, 2018).

Epidemiological data show that malaria cases are more prevalent in Africa, Asia and the Americas (Mishra et al. 2017). Despite presenting alarming rates and efforts to treat and eradicate this parasitosis, malaria

---

* Corresponding author.
E-mail address: iranildoj@gmail.com (I.J. da Cruz Filho).

https://doi.org/10.1016/j.exppara.2023.108498
Received 9 October 2022; Received in revised form 10 February 2023; Accepted 3 March 2023

was responsible for causing an approximate number of 214 million people infected with an estimate of almost half a million deaths related to this disease observed in the year 2015 (Ramsay et al., 2016).

Different compounds are used in the therapy of the parasitic diseases. Individuals affected with leishmaniasis are treated with pentavalent antimoniates, which are first-choice drugs, and amphotericin B and liposomal amphotericin B (Chattopadhyay and Jafurulla, 2011; Silva et al. 2020), pentamidine, paromycin, or miltefosine (Scariot et al. 2017; Silva et al. 2020) as second-choice drugs. For american trypanosomiasis, the available drugs are nifurtimox and benznidazole (García-Huertas and Cardona-Castro, 2021).

For *P. falciparum*, the drugs used are chloroquine, and for resistant strains, artemisinin and its derivatives are used (Achan et al., 2018). However, monotherapy for these parasites can lead to the emergence of drug resistance. Therefore, a promising alternative has been the use of therapeutic associations combining two or more compounds (Chattopadhyay and Jafurulla, 2011; Scariot et al. 2017; Silva et al. 2020).

However, the need to search for new antiparasitic derivatives becomes even more evident and necessary. Thus, some compounds have shown importance due to their therapeutic activity evaluated through several *in vitro* and *in vivo* studies (Silva et al. 2020; Jacob et al. 2021). In this context, thiosemicarbazones and thiazoles stand out, since their main characteristics are versatile, high yield and stability under different reaction conditions, as well as their wide applicability as intermediates of several important nuclei (Du et al. 2002; Tenório et al., 2005).

Literature data show that these classes a broad pharmacological profile, including antibacterial and antifungal activities (Kaplancıklı et al., 2016; Araújo-Neto et al. 2017; Volynets et al. 2019), antiviral (SantaCruz et al. 2017), anti-inflammatory and antinociceptive (Nam et al. 2017; Jacob et al. 2021), antiparasitic (Silva et al. 2020), antimalarial (Matsa et al. 2019) and besides being able to interact with biological macromolecules (DNA/HSA) (Alves et al. 2021a; Ribeiro et al. 2021). In addition, the selective activity of thiosemicarbazone -based derivatives has also been demonstrated on protozoa, among which the trypanocidal activities can be mentioned (Moraes Gomes et al. 2016), leishmanicidal (Scariot et al. 2017), and antimalarial (Matsa et al. 2019).

Thus, given all the difficulties pointed out and commented on about NTDs, this study aimed to obtain new compounds derived from thiosemicarbazones and thiazoles. In addition to a preliminary screening to evaluate their cytotoxic potential against mammalian cells and antiparasitic *in vitro* against *Leishmania* amazonensis (L. amazonensis), T. cruzi and P. falciparum, given its great importance in the world economy and public health.

2. Materials and methods

2.1. Reagents

All reagents used were obtained commercially (Merck, and Fluka): hydrazine (CAS 302-01-2), phenyl-isothiocyanate (CAS 103-72-0), 4-chlorophenyl-isothiocyanate (CAS 2131-55-7), 1-naphthyl isothiocyanate (CAS 551-06-4), 4-methoxyphenyl isothiocyanate (CAS 2284-20-0), 2-phenylethyl isothiocyanate (CAS 2257-09-2), allyl isothiocyanate (CAS 57-06-7), 4-nitrophenyl isothiocyanate (CAS 2131-61-5), 4-bromophenyl isothiocyanate (CAS, 1985-12-2), *p*-tolyl isothiocyanate (CAS 622-59-3), 3-pyridil isothiocyanate (CAS 15268-31-2), 4-fluorophenyl isothiocyanate, (CAS 1544-68-9), -naphthaldehyde (CAS 66-77-3), glacial acetic acid (CAS 64-19-7), dimethyl sulfoxide-d6 (CAS 2206-27-1), absolute ethanol (CAS 64-17-5), 2- bromoacetophenone (CAS 9870-11-1), 2-bromo-4′-chloroacetophenone (CAS 536-38-9), 2-bromo-4′-nitroacetophenone (CAS 43229-01-2), methanol (CAS 67–56 -1), 3-(4,5-dimethylthiazol-2-yl)-2,5-diphenyltetrazolium (MTT) (CAS 298-93-1), Griess reagent (Merck). Phosphate buffer saline (Merck), serum fetal bovine (Thermo Fisher Scientific), Schneider® culture medium (Merck), benznidazole (CAS 22994-85-0), chlorophenol red-β-D-galactopyranoside (CAS 99792-79-7), miltefosine (CAS 58066–85 -6), deuterated dimethyl sulfoxide (DMSO-d6) (CAS 67-68-5), RPMI 1640 culture medium (Thermo Fisher Scientific), gentamicin (Novafarma), fetal bovine serum (Thermo Fisher Scientific), Chloroquine (CAS 54–05 -7-7), AlbuMAXII (Invitrogen™), D-sorbitol (CAS 50-70-4). Nonidet P-40(Thermo Fisher Scientific).

2.2. Synthesis of thiosemicarbazone compounds

Thiosemicarbazones (1a – m) were obtained according to Oliveira et al. (2016) and Jacob et al. (2021) with adaptations. Initially, the synthesis of thiosemicarbazides was carried out from hydrazine hydrate (1 mmol) and equimolar amounts of substituted isothiocyanate in 20 mL of dichloromethane. The reaction was refluxed for 2 h at a temperature of 30 ± 5 °C. The product was filtered, washed with dichloromethane, and dried in a vacuum desiccator.

The thiosemicarbazides obtained (1 mmol) were reacted with substituted 3-indole-carboxaldehyde (1 mmol) in absolute ethanol (10 mL), using a catalytic amount of glacial acetic acid (0.75 mL). The reaction was run for 2 h at 30 ± 5 °C, followed by thin layer chromatography. The thiosemicarbazone-based derivates (1a - m) were precipitated from the reaction mixture, washed with absolute ethanol, and dried. The thiosemicarbazones (1 mmol) were reacted with 1-naphthaldehyde (1 mmol) in absolute ethanol (10 mL) using a catalytic amount of glacial acetic acid (0.75 mL). The reaction was run for 2 h at 30 ± 5 °C, also followed by thin layer chromatography (Merck, silica gel F254 on aluminum foil). The product was precipitated, washed with absolute ethanol and dried.

Then, the compounds (1a – m) were submitted to physicochemical characterization. Melting points were determined in capillary tubes with a Fisatom device (model 431D 60W, Brazil). The IR spectrum was generated using the Spectrum 400 equipment (Perkin Elmer) in KBr pellets. Mass spectrometry was performed using a MALDI-TOF Autoflex III device (Bruker Daltonics, USA). NMR spectra were obtained using Bruker AMX-300 MHz devices (300 MHz for ^{1}H and 75.5 MHz for ^{13}C) or Varian UnityPlus 400 MHz spectrometer (400 MHz for ^{1}H and 100 MHz for ^{13}C). The physicochemical characterization is described in the Supplementary material (S1).

2.3. Synthesis of 1,3-thiazole compounds

The thiosemicarbazones (1a – m) (0.25 mmol) were subjected to Hantzsch condensation with equimolar amounts (0.25 mmol) of some acetophenones: 2-bromoacetophenone, 2-bromo-4′-chloroacetophenone, 2-bromo-4′-nitroacetophenone (Alves et al. 2021a). The reaction was carried out in ethanol (10 mL) for 2 h, at reflux, being monitored by thin layer chromatography. The precipitated product (thiazole 2a – p) was filtered, washed with absolute ethanol, and dried. Finally, the compounds (2a – p) were submitted to physicochemical characterization, using the same analyzes performed for the thiosemicarbazone compounds. The physicochemical characterization is described in the Supplementary material (S2).

Fig. 1 shows the synthesis diagram for obtaining the thiosemicarbazone and thiazole compounds evaluated in this study.

2.4. In silico analysis of pharmacokinetic parameters

The absorption, distribution, metabolism, and excretion (ADME) profiles of the synthesized compounds were evaluated by two free platforms; SwissADME (http://www.swissadme.ch/) and pkCSM (http://biosig.unimelb.edu.au/pkcsm/prediction) (Pires et al., 2015; Daina et al., 2017). The parameters assessed were: molecular mass, hydrogen bond acceptors, hydrogen bond donors, log P, TPSA, LogS, permeability in Caco-2, intestinal absorption, the volume of distribution, fraction not bound to serum proteins, and total clearance. These *in*

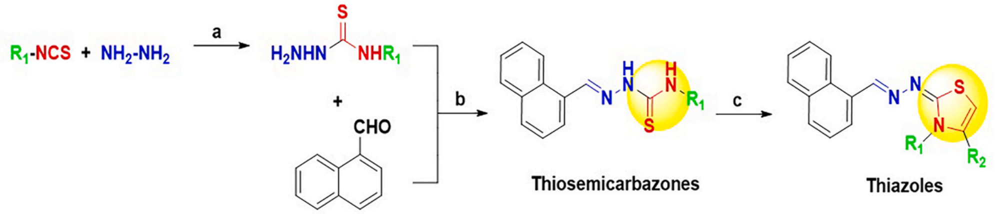

Compound	R_1
1a	H
1b	allyl
1c	Phenyl
1d	4-methylphenyl
1e	4-ethylphenyl
1f	4-methoxyphenyl
1g	2-phenethyl
1h	4-fluorophenyl
1i	4-chlorophenyl
1j	4-bromophenyl
1k	4-nitrophenyl
1l	3-pyridyl
1m	1-naphthyl

Compound	R_1	R_2	Compound	R_1	R_2
2a	allyl	phenyl	2n	4-fluorophenyl	4-nitrophenyl
2b	Phenyl	phenyl	2o	4-chlorophenyl	4-nitrophenyl
2c	4-methylphenyl	phenyl	2p	4-nitrophenyl	4-nitrophenyl
2d	4-methoxyphenyl	phenyl			
2e	3-pyridyl	phenyl			
2f	1-naphthyl	phenyl			
2g	H	4-nitrophenyl			
2h	allyl	4-nitrophenyl			
2i	Phenyl	4-nitrophenyl			
2j	4-methylphenyl	4-nitrophenyl			
2k	4-ethylphenyl	4-nitrophenyl			
2l	4-methoxyphenyl	4-nitrophenyl			
2m	2-phenethyl	4-nitrophenyl			

Fig. 1. Structures of thiosemicarbazones and thiazole derivatives.

silico assays were performed to predict the behavior of these compounds' *in vitro* assays.

2.5. Preparation of solutions of compounds to perform biological assays

To carry out the assays, the compounds were solubilized in dimethylsulfoxide (DMSO) to obtain a stock concentration of 800 μM. Then, they were diluted in different concentrations. Dilutions were performed with phosphate buffered saline to obtain a final concentration of 1% DMSO.

2.6. In vitro antioxidant activity: ABTS radical scavenging assay

The antioxidant activity of the compounds was determined by the free radical scavenging method 2,2′-azino-bis (3-ethylbenzothiazolin-6-sulfonic acid) (ABTS) (Jaishree et al. 2012; Mic et al. 2021). The ABTS + radical was produced from the reaction of an aqueous solution of ABTS (7 mM) with potassium persulfate (140 mM). The solution was kept in the absence of light, at 25 °C for 16 h and then diluted in ethanol until an absorbance of 0.75 ± 0.05 nm at a wavelength of 734 nm was obtained. Compounds were diluted at concentrations ranging from 7.9 to 1000 μg/mL.

The assays consisted of 100 μL of the respective compounds and 3.9 mL of the ABTS solution. The experimental standards were ascorbic acid and BHT at the same concentrations as the compounds. Assays were kept in the dark for 15 min. Further, they were analyzed in a UV–Vis spectrophotometer (Shimadzu UV-2550). The experimental blank was absolute ethanol. All experiments were performed in triplicate. The percentage of capture was determined according to Equation (1).

$$\text{ABTS }\% = \left(\frac{A_c - A_s}{A_c}\right) * 100\% \tag{1}$$

Where Ac = Control absorbance; As = Sample absorbance.

With the results, it was possible to obtain a curve of the antioxidant activity (dose-response) as a function of the concentration of the compounds. The IC_{50}, (concentration that captures 50% of ABTS radicals) was determined by nonlinear regression.

2.7. Fluorescent emission spectroscopy

2.7.1. Interaction assays of compounds with bovine serum albumin (BSA)

Interaction assays with BSA have been proposed by Alves et al. (2021b) and Ribeiro et al. (2021). BSA was dissolved in 10 mL of Tris-HCl buffer (0.1 M, pH 7.6) to obtain a concentration of 10 μM. After preparing the solution, it was stored at a temperature of −20 °C, to be reused later. The concentrations of the samples referring to the test solutions were varied in 5, 10, 15, 20, 25, 30, 35, and 40 μM. Then, the different concentrations were added to albumin (1 mL). The systems were homogenized and left at room temperature for 10 min for stabilization in the buffer and, later, subjected to fluorescence analysis. Emission spectra were recorded in the region of 310–400 nm using an excitation wavelength of 285 nm, with excitation and emission bands of 2.5 nm. All determinations were carried out at room temperature (25 °C) in a rectangular quartz cuvette with a length of 1 cm.

The emission suppression behavior was analyzed using the Stern-Volmer Equation (2) (Ksv).

$$\frac{F_0}{F} = 1 + K_q\tau_0[Q] = 1 + K_{sv}[Q] \tag{2}$$

Where F_0 and F are the fluorescence intensities in the absence and presence of the compound, respectively, K_{SV} is the SternVolmer constant, [Q] is the concentration of the ligand, K_q is the biomolecular suppression constant and τ_0 is the half-life in the absence of the compound (10^{-8}s). The graph of relative emission intensity (F_0/F) versus [Q] was used to obtain the constant from the linear regression of the graph. Binding data was obtained from SigmaPlot 10.0 software.

2.7.2. Interaction assays of compounds with DNA

The interaction study of compounds with DNA was performed by Alves et al. (2021b) containing few modifications. For this, Tris-HCl buffer solution (50 mM, pH = 7.4) with 100 mM NaCl was used to adjust the ionic strength. A stock solution of ssDNA was carried out in a buffer. To assess whether the nucleic acid was free of protein, the absorbance was determined (in a Shimadzu UV-2550 spectrophotometer) at 260 and 280 nm, where the ratio absorbance 260 nm/absorbance 280 nm = 1.8–1.9, indicates that the macromolecule is without contamination. Subsequently, the determination of the ssDNA concentration was performed using the Lambert-Beer equation, using the absorbance at 260 nm, with a molar extinction coefficient of 6600 L/mol and an optical path of 1 cm.

For studies using fluorimetric titration (Shimadzu spectrofluorimeter, model RF 5301), the concentration and volume of ssDNA were kept constant (10 μmol/L and 1.0 mL) and the compounds were added in increasing amounts, in concentrations ranging from 5 to 40 μmol/L (10 μL volume). In the assays to evaluate the binding mode with ctDNA, a stock solution of ethidium bromide at 0.5 mmol/L was used with instrumental parameters λex = 520 nm and λem = 598 nm. All experiments were performed in triplicate.

The emission suppression behavior was analyzed using the Stern-Volmer Equation (2) (Ksv). The graph of relative emission intensity (F0/F) versus [Q] was used to obtain the constant from the linear regression of the graph. Binding data were obtained from SigmaPlot 10.0 software.

2.8. *Cytotoxic activity against mammalian cells*

Cytotoxicity on macrophage (RAW 264.7), Chinese hamster lung fibroblasts (V79), and hepatoma (HepG2) cells were evaluated by 3-(4,5-dimethylthiazol-2-yl)-2 bromide tests, 5-diphenyltetrazolium (MTT) (Santos-Silva et al. 2016; Queiroz et al. 2020; Silva et al. 2020).

Cells were seeded in 96-well plates (1×10^{6} cells/well) containing RPMI medium with phenol red supplemented and incubated in a 5% CO_2 atmosphere at 37 °C. After 24 h, the cells were incubated in the presence of various concentrations of the compounds (200–6 μM) in an atmosphere of 5% CO_2 and 37 °C for 72 h. At the end of the incubation period, 10 μL of MTT at a concentration of 5 mg/mL was added to the cell culture wells, and after 3 h of incubation with MTT, 50 μL of DMSO were added to dissolve the Formazan blue crystals. The absorbance reading of formazan crystals was determined using a Benchmark Plus plate reader (Bio-Rad, California, USA) at a wavelength of 540 nm.

The experimental control consisted of only cells grown in a culture medium. The experimental standards used were: miltefosine, amphotericin B, benznidazole, and chloroquine, under the same conditions as the compounds. Cell viability and growth inhibition were calculated using Equations (3) and (4) respectively.

$$\text{Cell viability } (\%) = \left(\frac{VC}{TC}\right) * 100\% \tag{3}$$

$$\text{Inhibition } (\%) = 100 - \text{cell viability} \tag{4}$$

Where: VC is the number of cells at different concentrations, TC is the concentration of cells in the control which represents 100% viability.

The cytotoxic concentration that inhibits 50% of cell growth (CC_{50}) for all cells evaluated was determined by non-linear regression using GraphPad Prism 5 software (test version). The experiments were performed in triplicate.

2.8.1. *In vitro hemolytic activity*

Hemolytic activity assays were performed to assess toxicity against erythrocytes (Queiroz et al. 2020). Initially, compounds in RPMIc were incubated in healthy 0Rh + erythrocytes. A 3% HTC suspension of RBCs in the RPMIc culture medium was grown for 72 h under standard culture conditions (37 °C, 5% CO_2, and 90% N_2) in the presence of a serial dilution of 1: 3 of each compound, ranging from 200 to 6 μM. The suspension without any standard or study compounds and in the presence of a 20% Triton™-X solution was applied as negative (0% hemolysis) and positive (100% hemolysis) controls, respectively.

After 72 h, the cells were centrifuged at 2000 rpm/5 min and the supernatant was used to assess hemolytic activity by quantifying the release of hemoglobin, via spectrophotometric absorbance measurement at 450 nm with a Multimode microplate reader (Triad, Dynex Technologies). The average percentage of hemolysis was calculated from two independent experiments, each in triplicate, using Microsoft Excel software, through Equation (5). Where the average absorbance of the negative control was subtracted from the sample and the average absorbance of the positive control remove the background absorbance readings.

$$\%\ \text{Hemolysis} = \frac{(\text{Sample absorbance} - \overline{X}\text{Negative Control absorbance})}{(\overline{X}\text{Positive Control absorbance} - \overline{X}\text{Negative Control absorbance})} \times 100 \tag{5}$$

In general, any compound below 10% hemolysis is non-hemolytic, while values above 25% hemolysis are classified as hemolytic (Amin and Dannenfelser, 2006). The experimental standards used were: miltefosine, amphotericin B, benznidazole, and chloroquine under the same experimental conditions as the compounds. This study was approved by the Ethics Committee for the Use of Animals of the Institute Aggeu Magalhães/Foundation Oswaldo Cruz, protocol number 164/2020. The experiments were performed in triplicate and two independent experiments.

2.9. *Evaluation of leishmanicidal activity in vitro*

2.9.1. *Antipromastigote activity*

The tests were performed according to Silva et al. (2020), Queiroz et al. (2020), Zuma et al. (2021) and Freitas et al. (2021) with modifications. Promastigote forms of *Leishmania amazonensis* (strain WHOM/00 LTB 0016) were maintained at 26 °C in Schneider culture medium supplemented with 10% fetal bovine serum (complete medium). Parasites in the exponential phase (72 h) of growth were used in all experiments. For the leishmanicidal activity assay, the parasites were cultured in Schneider medium and counted up to a concentration of 1×10^{6} cells/mL. Then the parasites were incubated at 26 °C in the presence of different concentrations of the compounds (0.19–400 μM) for 72 h.

Parasites in the exponential phase (72 h) of growth were used in all experiments. For the leishmanicidal activity assay, the parasites were cultured in Schneider medium and counted up to a concentration of 1×10^{6} cells/mL. Then the parasites were incubated at 26 °C in the presence of different concentrations of the compounds (0.19–400 μM) for 72 h. Parasites incubated only with culture medium and Miltefosine and Amphotericin B were used as negative and positive controls, respectively. Cell growth was assessed and IC_{50}/72 h was determined by non-linear regression analysis using GraphPad Prism 5 software (trial version). The experiments were performed in triplicate and two independent experiments.

2.9.2. *Anti-amastigote activity*

The tests were carried out using the methodology proposed by Zuma et al. (2021) and Freitas et al. (2021). For this evaluation, RAW 264.7 macrophages were distributed in 24-well plates (3×10^{5} cells/mL) containing a sterile round coverslip. Macrophages were incubated for adhesion for 2 h at 37 °C and 5% CO_2 atmosphere.

After the initial incubation, the promastigote forms of *L. amazonensis* were added to the macrophage culture in the proportion of 8 parasites/macrophage, for 6 h, at 37 °C and 5% CO_2. Non-internalized parasites were removed by washing and the culture was incubated again in the presence of different concentrations of the compounds (0.19–400 μM) for 24 h, at 37 °C and 5% CO_2. Miltefosine and Amphotericin B were used as positive control, at the same concentrations as the compounds. After the incubation, the coverslips containing the culture were washed with PBS, collected, and stained with the Panoptic Rapid staining kit. The percentage of infected macrophages as well as the number of amastigotes/macrophages was determined by counting 100 macrophages in duplicate. The leishmanicidal activity promoted by the compounds was evaluated by the decrease in the number of infected macrophages and intracellular amastigotes in the treated cultures compared to the untreated control culture. IC_{50} values were calculated by regression analysis using GraphPad Prism software. The experiments were performed in triplicate.

2.10. Evaluation of in vitro trypanocidal activity

2.10.1. Anti-trypomastigote activity

Anti-trypomastigote activity was evaluated according to Freitas et al. (2021) with adaptations. To evaluate the anti-trypanosomal activity, trypomastigote forms derived from *T. cruzi* cells, Tulahuen strain stably expressing the β-galactosidase gene from *Escherichia coli* (Tulahuen-lacZ), 1.0×10^5 trypomastigotes, were cultured in plates. 96 wells containing RPMI 1640 medium without phenol red plus 10% fetal bovine serum and glutamine. Plates were incubated for 4 days at 37 °C with compounds (diluted in 1% DMSO) at serial concentrations ranging from 0.19 to 400 μM. After incubation, a solution of 50 μL of CPRG (Chlorophenol red-β-D-galactopyranoside, 500 μM, 0.5% Nonidet P-40, in PBS) was added and the plates were incubated again for 4 h at 37 °C and subsequently the absorbances were determined at 570 nm. The parasite viability results were measured based on the catalysis of CPRG by β-galactosidase. IC_{50} values were obtained using GraphPad Prism software. All experiments were performed in triplicate using benznidazole as a positive control. The experiments were performed in triplicate.

2.10.2. Anti-amastigote activity

The anti-amastigote activity was initially investigated by Zuma et al. (2021) and Freitas et al. (2021) with very few adaptations. To obtain the amastigote forms of *T. cruzi* (Tulahuen strain), macrophage cells (RAW 264.7) were seeded in a 96-well plate and incubated at 37 °C in 5% CO_2 atmosphere for 24 h. Parasites were added (10 trypomastigotes/RAW 264.7 cell), and after 3 h of interaction the non-internalized parasites were removed. The plates were incubated for 48 h for infection, after which the compounds were added at six concentrations (0.19–400 μM) and the cells were kept under the conditions described above for 96 h. After incubation, a solution of 50 μL of CPRG (Chlorophenol red-β-D-galactopyranoside, 500 μM, 0.5% Nonidet P-40, in PBS) was added and the plates were incubated for 18 h at 37 °C. The absorbance reading was performed in a Thermo Scientific Multiskan FC spectrophotometer at 570 nm.

Parasite viability results were measured based on β-galactosidase catalysis of CPRG and IC_{50} values were obtained using GraphPad Prism software. All experiments were performed in triplicate using benznidazole as a positive control. The experiments were performed in triplicate.

2.11. Determination of selectivity and specificity indices for each of the compounds evaluated.

The selectivity index (SI) is the relationship between the cytotoxicity of the compound for mammalian cells and its leishmanicidal and/or trypanocidal activities. It was calculated from the ratio between macrophage cytotoxicity (CC_{50}) and activity against amastigotes (IC_{50}). The specificity index (SPI) is defined as the ratio of the IC_{50} of the promastigote or trypomastigote forms and the IC_{50} of the amastigote forms (Santos Silva et al., 2017; Queiroz et al. 2020; Silva et al. 2020).

2.11. Anti-Plasmodium falciparum activity

The experiments were performed with the chloroquine-sensitive strain *P.* falciparum 3D7HT-GFP (Santos et al., 2015; Balabadra et al., 2017). The parasites were cultured at 5% hematocrit, 37 °C and 5% CO_2 atmosphere, human serum was replaced by 0.5% AlbuMAXII (Invitrogen™) in the culture medium. Synchronized cultures were obtained by consecutive treatments at 48 h intervals with 5% (w/v) D-sorbitol solution.

All compounds were evaluated for their *in vitro* antimalarial activity against strain 3D7 of *P. falciparum*. An unsynchronized culture with 1% hematocrit and 0.6% parasitaemia was incubated (37 °C and 5% CO_2) with the tested compounds in 3-fold serial dilutions ranging from 10 to 0.014 μM for 72 h. Compounds were dissolved in DMSO. Parasite growth was assessed by flow cytometry (Beckman Coulter, Cytoflex) with a 96-well plate reader, using Fl-1 (green fluorescent protein [GFP]; excitation wavelength, 488 nm). Typically, 20,000 to 40,000 RBCs were counted for each well.

The effective concentration promoting 50% inhibition of parasite growth (IC_{50}) was determined by non-linear regression using GraphPad Prism 5 software (trial version).

2.12. Statistical analysis

Linear regression analyzes were performed using the SPSS 18.0 program (IBM Co., New York, USA) for Windows. Significance analysis, considered significant p-values <0.05, was performed using the ANOVA test and Tukey's post-test in the GraphPad Prism 5.0 program (Graphpad, California, USA) for Windows.

3. Results and discussion

3.1. In silico study of the pharmacokinetic properties of thiosemicarbazones and thiazoles

One way to investigate the pharmacokinetic properties of a drug candidate compound is through *in silico* ADME studies (Pires et al., 2015; Daina et al., 2017). This information helps in the prediction of effects that may occur *in vitro* and *in vivo* studies (Lipinski et al., 1997a; Chen et al. 2020).

A theoretical study of thiosemicarbazones (1a-m) and their respective thiazoles (2a-p) (Fig. 1), was elaborated applying Lipinski's "rule of five" (log P, molecular mass, hydrogen bond acceptors and carbon donors). Hydrogen bonds) and determination of the topological surface area of the polar surface (TPSA) proposed by Veber (Lipinski et al., 1997b; Pires et al., 2015; Daina et al., 2017; Chen et al. 2020).

In addition to these, the parameters proposed by Pires et al. (2015) which we can mention: permeability in Caco-2 cells, intestinal absorption, the volume of distribution, unbound fraction, and total clearance (depuration). Table 1 presents the ADME results for all compounds synthesized in this study.

The results obtained showed that the thiosemicarbazones obeyed the parameters established by Lipinski (log $P \leq 5$, Molecular Mass $\leq$500, hydrogen bond acceptors $\leq$10, and hydrogen bond donors $\leq$5) and Veber (TPSA $\leq$140 Å2), suggesting probable good oral bioavailability.

However, cyclization of the thiosemicarbazones to the respective thiazoles resulted in the violation of one of the parameters of Lipinski's rule (logP for most compounds) and TPSA Veber's rule for compound 2p. Violation of one of the established parameters does not necessarily prevent the activity of the drug orally, since compounds that bind to biological transporters may be an exception to the rule (Lipinski et al., 1997b; Pires et al., 2015; Daina et al., 2017; Chen et al. 2020).

Another important parameter for the study of absorption is solubility, which is usually expressed by LogS, where S is the concentration of the compound in a saturated aqueous solution at equilibrium (Gouveia et al. 2022). According to Pires et al. (2015) compounds can be ranked in the following order of solubility: logS = insoluble < −10 < slightly soluble < −6 < moderately soluble < −4 soluble < −2 < very soluble <0 < highly soluble.

The results show that the thiosemicarbazones presented logS values between −6.86 and −3.83, being classified as soluble to sparingly soluble. The compound with the highest water solubility was compound 1a (logS = −3.83), while the compound with the lowest water solubility was 1m (logS = −6.86), which has a highly hydrophobic second group (R_1 = naphthyl), which decreases the water solubility of the molecule as a whole (Ribeiro et al. 2019).

On the other hand, the cyclization of thiosemicarbazones in thiazoles resulted in a reduction of the aqueous solubility of these compounds, verified by the lower values of logS (between −9.39 and −6.87). The thiazoles were classified as poorly soluble in water. Among the series of

Table 1
In silico pharmacokinetic data estimated at SwissADME or pkCSM webservice.

Comp.	R1	R2	MW (g/mol)[a]	HBA[b]	HBD[c]	log*P*[d]	TPSA (Å^2)[f]	log*S*[e]	Caco-2 perm.[g]	Int. abs. (%)[h]	VDSS (log L/kg)[i]	Fract. Unb.[j]	Total clearance (log mL/min/kg)[k]
1a	H	–	229.30	1	2	2.10	82.50	−3.83	1.27	92.04	0.51	0.16	−0.007
1b	Allyl	–	269.36	1	2	2.81	68.51	−4.61	1.43	93.20	0.72	0.11	0.12
1c	phenyl	–	305.40	1	2	3.66	68.51	−5.57	1.55	90.86	0.25	0	−0.07
1d	4-methylphenyl	–	319.42	1	2	3.89	68.51	−5.94	1.39	90.98	0.31	0	−0.13
1e	4-ethylphenyl	–	333.45	1	2	4.12	68.51	−6.40	1.55	87.93	0.45	0	−0.17
1f	4-methoxyphenyl	–	335.42	2	2	3.31	77.74	−5.73	1.41	89.66	0.20	0	−0.04
1g	2-phenylethyl	–	333.45	1	2	3.85	68.51	−5.98	1.55	92.36	0.47	0	−0.04
1h	4-fluorophenyl	–	323.39	2	2	4.05	68.51	−5.67	1.34	90.52	0.17	0	−0.22
1i	4-chlorophenyl	–	339.84	1	2	4.16	101.84	−6.22	1.53	87.82	0.30	0	−0.21
1j	4-bromophenyl	–	384.29	1	2	4.28	68.51	−6.28	1.01	87.75	0.31	0	−0.23
1k	4-nitrophenyl	–	350.39	3	2	2.65	114.33	−6.35	0.42	86.78	0.19	0	−0.06
1l	3-pyridyl	–	306.38	2	2	2.18	81.40	−4.73	1.37	93.08	0.36	0.08	0.061
1m	1-naphthyl	–	355.46	1	2	4.39	68.51	−6.86	0.94	91.80	−0.151	0	−0.016
2a	Allyl	phenyl	369.48	2	0	4.28	57.89	−6.87	1.02	93.57	0.42	0.14	0.39
2b	phenyl	phenyl	405.51	2	0	5.03	57.89	−7.82	1.06	94.61	0.12	0.23	0.25
2c	4-methylphenyl	phenyl	419.54	2	0	5.24	57.89	−8.20	1.05	94.76	0.10	0.24	0.20
2d	4-methoxyphenyl	phenyl	435.54	3	0	4.65	67.12	−7.99	1.07	95.13	0.04	0.24	0.29
2e	3-pyridyl	phenyl	406.50	3	0	3.98	70.78	−6.98	1.14	99.42	0.63	0.24	0.39
2f	1-naphthyl	phenyl	455.57	2	0	5.66	57.89	−9.12	1.06	98.64	−0.23	0.29	0.41
2g	H	4-nitrophenyl	374.42	4	1	3.49	114.57	−7.03	0.50	92.26	0.06	0	0.24
2h	Allyl	4-nitrophenyl	414.48	4	0	4.08	103.71	−7.65	0.43	95.81	0.45	0.10	0.29
2i	phenyl	4-nitrophenyl	450.51	4	0	4.84	103.71	−8.61	0.29	96.51	0.001	0.24	0.16
2j	4-methylphenyl	4-nitrophenyl	464.54	4	0	5.04	103.71	−8.98	0.36	96.45	0.05	0.24	0.11
2k	4-ethylphenyl	4-nitrophenyl	478.56	4	0	5.24	103.71	−9.43	0.29	96.37	−0.002	0.24	0.07
2l	4-methoxyphenyl	4-nitrophenyl	480.54	5	0	4.51	112.94	−8.77	0.38	97.41	−0.01	0.25	0.20
2m	2-phenylethyl	4-nitrophenyl	478.56	4	0	4.97	103.71	−9.02	0.27	95.72	0.15	0.19	0.16
2n	4-fluorophenyl	4-nitrophenyl	468.50	5	0	5.21	103.71	−8.71	0.34	95.95	−0.05	0.26	0.02
2o	4-chlorophenyl	4-nitrophenyl	484.96	4	0	5.31	103.71	−9.26	0.31	95.00	0.06	0.24	0.03
2p	4-nitrophenyl	4-nitrophenyl	495.51	6	0	3.96	149.53	−9.39	0.47	100	−0.43	0.25	0.18

[a] SwissADME Molecular Weight.
[b] SwissADME Number H-bonds acceptors.
[c] SwissADME Number H-bonds donors.
[d] SwissADME Moriguchi log of octanol-water partition coefficient.
[e] SwissADME Ali log of aqueous solubility.
[f] SwissADME calculation of Topological Polar Surface Area (TPSA).
[g] pkCSM prediction of Caco-2 cell permeability as estimation of absorption at human intestinal mucosa.
[h] pkCSM prediction of the proportion of compound absorption though the human small intestine.
[i] pkCSM prediction of the log of steady state volume of distribution (VDss).
[j] pkCSM prediction of compound fraction unbound in plasma (not bound to serum proteins).
[k] pkCSM prediction of the log of total drug clearance.

thiazole derivatives, the solubility increased in the following order: R_2 = 4-nitrophenyl (logS between −9.91 and −7.03) < phenyl (logS between −9.12 and −6.87).

Although the polar group R_2 = 4-nitrophenyl conferred lower lipophilicity in the series of thiazole derivatives (MlogP = 3.49–5.47), it was responsible for the lower aqueous solubility in the three series of thiazoles investigated, contrary to what might be expected.

A possible explanation is that, in solid compounds, the presence of groups that strongly donate or accept hydrogen bonds (the latter being the nitro group category) can help to stabilize the crystal lattice through the formation of hydrogen bonds. This leaves the compound less susceptible to attack and solubilization by water (Raevsky et al., 2004), consequently, there is a reduction in the aqueous solubility of the nitrocompounds.

Other important properties for compounds with pharmaceutical potential were investigated through the pkCSM platform, such as the human colon adenocarcinoma cell line, Caco-2, which allows the evaluation of the potential capacity of *in vivo* intestinal absorption of drugs, in addition to allowing the determination of transport mechanisms of a vast number of drug candidate molecules (Lipinski et al., 1997a; Pires et al., 2015; Daina et al., 2017; Chen et al. 2020). Thus, compounds with values $< 1.10^{-6}$ cm s^{-1} are poorly absorbed, between 1 and 10.10^{-6} cm s^{-1} are moderately absorbed, and $>10.10^{-6}$ cm s^{-1} are well absorbed (Pires et al., 2015). Thiosemicarbazones and triazoles, according to the values in Table 1, may show absorption ranging from moderate to low compared to Caco-2.

Intestinal absorption percentage is a method built to predict the proportion of compounds that have been absorbed by the human small intestine (Gouveia et al. 2022). Normally, the intestine is the site for the absorption of a drug from an orally administered solution (Pires et al., 2015; Gouveia et al. 2022). The compounds analyzed in this work showed an interesting percentage of absorption through the small intestine, presenting results greater than 70% (Pires et al., 2015).

Another factor observed was the volume of distribution (VDss), which is the theoretical volume that the total dose of a drug would need to be uniformly distributed so that it gives the same concentration as in blood plasma (Pires et al., 2015; Gouveia et al. 2022). VDss values indicate the volume of distribution of the compound where VDss values > 0.45 indicate that the compound is more likely to be distributed into tissues than into plasma. The values showed a value of log VDss < -0.15 and this indicates that the ligands are more likely to be distributed in plasma than in tissues (Ribeiro et al. 2019; Gouveia et al. 2022). Thiosemicarbazones in general are likely to be more readily distributed in tissues than plasma, except compound 1m which had to log VDss < -0.15, being distributed in plasma. Most of thiazoles-based derivatives also showed greater distribution in tissue, however, compounds 2f, 2k, 2l, 2n, and 2p are more likely to be distributed in plasma.

These compounds presented low fraction not bound to proteins. An important feature, since the increase in the free fraction, can lead to an increase in its distribution to tissues and organs, perhaps, an increase in toxicity (Pires et al., 2015; Gouveia et al. 2022). Finally, there is the total clearance (Total clearance). A drug with a high total release value will present a rapid excretion process and consequently a shorter action time (Pires et al., 2015; Moraes Gomes et al. 2016; Gouveia et al. 2022). This profile was not observed in the compounds under study, since the release values ranged from -0.007 to 0.41 log mL/min/kg.

3.2. *In vitro antioxidant activity*

The thiosemicarbazone and thiazole compounds are described in the literature as promoting different biological activities (Ali and Sayed, 2021; Kanso et al. 2021). These activities are directly related to the chemical structure of these compounds (Jadhav et al. 2021). The *in vitro* antioxidant activities of all synthesized compounds were evaluated by the ABTS assay, a fast and efficient methodology to perform an initial screening of the antioxidant potential of different compounds (Salar et al. 2019). IC_{50} values for each of the compounds are shown in Table 2.

The results presented in Table 2 showed that the thiosemicarbazones presented higher results of antioxidant activity when compared to the thiazole compounds. The thiosemicarbazones presented IC_{50} ranged from 17.9 to 127.5 μM. On the other hand, the thiazoles presented IC_{50} values that ranged from 37.6 to values greater than 1830.3 μM respectively.

The compounds were considered strong antioxidants when $IC_{50} < 80$ μM moderate from 80 to 200 μM and above 200 μM weak antioxidant power. Therefore, we will only evaluate the compounds that showed high antioxidant activity. Compounds with lower IC_{50} are considered more antioxidant. Among the compounds that were considered as strong antioxidants, we can classify them in order of strength: 1f > 1b > 1 k > 1i > 2g > 1d > 1g > 1m > 1c > 1j, respectively.

The three substituents that promoted greater activities were 4-methoxyphenyl followed by allyl and 4-nitrophenyl substituents. These substituents are already described in the literature for promoting promising antioxidant activity. Salar et al. (2019) obtained hybrid scaffolds based on coumarin substituted with hydrazinyl thiazole and obtained IC_{50} results ranging from 0.37 to 1.844 μM for the ABTS assay. Yildiz et al. (2022) evaluated different thiosemicarbazones based on dimethoxy-indoles, they obtained IC_{50} ranging from 17.38 to 96.10 μM. These results reinforce that the antioxidant activity is directly related to the chemical structure of the compounds.

3.3. *Interaction assays between compounds with albumin and with DNA*

Serum albumins play an important role in the transport of molecules through the bloodstream (Alves et al. 2021a; Ribeiro et al. 2021). Therefore, studies are carried out to evaluate whether the interaction of these proteins with different drugs can promote damage to these proteins, causing loss of function (Alves et al. 2021a). Table 3 presents the interaction results for each of the compounds obtained.

The results presented in Table 3 showed that the thiosemicarbazones showed higher results of interaction with albumin when compared to the thiazole compounds. The thiosemicarbazones presented Ksv that ranged from 3.5×10^3 to 4.6×10^6 (M^{-1}). On the other hand, the thiazoles presented Ksv values that ranged from 2.6×10^3 to 2.0×10^5 respectively. Thus, the compounds were able to interact with albumin weakly (1×10^3 to 1×10^4 M^{-1}), moderate (1×10^4 to 1×10^5 M^{-1}), and high (1×10^5 to 1×10^6 M^{-1}) (Silva Filho et al. 2019; Wang et al. 2021; Szymaszek et al. 2022). In addition to albumin interaction assays, DNA interaction assays were performed. DNA interaction results are shown in Table 4.

The results in Table 4 demonstrate that thiosemicarbazones and thiazoles presented values ranging from 1.1×10^3 to 9.0×10^4 (M^{-1}). These values indicate that the synthesized compounds can moderately to poorly interact with DNA. The literature presents works that have

Table 2

In vitro antioxidant activity promoted by the compounds.

Compound	R_1	R_2	ABTS IC_{50} (μM)
1a	H	–	122.8 ± 1.0
1b	Allyl	–	23.6 ± 0.1
1c	phenyl	–	48.0 ± 2.0
1d	4-methylphenyl	–	40.5 ± 1.3
1e	4-ethylphenyl	–	80.5 ± 0.1
1f	4-methoxyphenyl	–	17.9 ± 1.1
1g	2-phenylethyl	–	42.1 ± 0.6
1h	4-fluorophenyl	–	127.5 ± 1.0
1i	4-chlorophenyl	–	36.1 ± 0.2
1j	4-bromophenyl	–	58.7 ± 0.1
1k	4-nitrophenyl	–	34.1 ± 1.1
1l	3-pyridyl	–	87.2 ± 0.2
1m	1-naphthyl	–	43.1 ± 0.0
2a	Allyl	Phenyl	>1000
2b	phenyl	phenyl	>1000
2c	4-methylphenyl	phenyl	>1000
2d	4-methoxyphenyl	phenyl	>1000
2e	3-pyridyl	phenyl	1830.3 ± 0.3
2f	1-naphthyl	phenyl	1746.6 ± 0.5
2g	H	4-nitrophenyl	37.6 ± 0.7
2h	Allyl	4-nitrophenyl	>1000
2i	phenyl	4-nitrophenyl	>1000
2j	4-methylphenyl	4-nitrophenyl	>1000
2k	4-ethylphenyl	4-nitrophenyl	>1000
2l	4-methoxyphenyl	4-nitrophenyl	>1000
2m	2-phenylethyl	4-nitrophenyl	>1000
2n	4-fluorophenyl	4-nitrophenyl	>1000
2o	4-chlorophenyl	4-nitrophenyl	>1000
2p	4-nitrophenyl	4-nitrophenyl	285.7 ± 2.0
Ascorbic acid	–	–	76.9 ± 0.3
Butylated hydroxytoluene	–	–	28.6 ± 0.1

Mean ± SEM.

Table 3
The interaction of compounds with bovine serum albumin (BSA).

Compound	R_1	R_2	Ksv (M^{-1})
1a	H	–	$2.1 \times 10^5 \pm 0.2$
1b	Allyl	–	$2.0 \times 10^6 \pm 1.1$
1c	phenyl	–	$3.5 \times 10^3 \pm 1.6$
1d	4-methylphenyl	–	$1.4 \times 10^4 \pm 2.2$
1e	4-ethylphenyl	–	$4.6 \times 10^6 \pm 0.1$
1f	4-methoxyphenyl	–	$4.6 \times 10^3 \pm 0.4$
1g	2-phenylethyl	–	$2.2 \times 10^4 \pm 0.3$
1h	4-fluorophenyl	–	$2.2 \times 10^4 \pm 0.1$
1i	4-chlorophenyl	–	$1.4 \times 10^4 \pm 0.9$
1j	4-bromophenyl	–	$1.9 \times 10^4 \pm 0.1$
1k	4-nitrophenyl	–	$1.0 \times 10^5 \pm 0.7$
1l	3-pyridyl	–	$1.5 \times 10^5 \pm 0.9$
1m	1-naphthyl	–	$2.0 \times 10^5 \pm 0.1$
2a	Allyl	phenyl	$9.0 \times 10^4 \pm 0.2$
2b	phenyl	phenyl	$1.0 \times 10^5 \pm 1.1$
2c	4-methylphenyl	phenyl	$4.1 \times 10^4 \pm 1.2$
2d	4-methoxyphenyl	phenyl	$2.0 \times 10^5 \pm 1.4$
2e	3-pyridyl	phenyl	$1.6 \times 10^5 \pm 0.0$
2f	1-naphthyl	phenyl	$3.6 \times 10^4 \pm 0.1$
2g	H	4-nitrophenyl	$1.8 \times 10^4 \pm 0.8$
2h	Allyl	4-nitrophenyl	$3.8 \times 10^4 \pm 0.7$
2i	phenyl	4-nitrophenyl	$4.1 \times 10^4 \pm 1.5$
2j	4-methylphenyl	4-nitrophenyl	$6.7 \times 10^4 \pm 1.1$
2k	4-ethylphenyl	4-nitrophenyl	$3.4 \times 10^3 \pm 1.3$
2l	4 methoxyphenyl	4-nitrophenyl	$1.0 \times 10^4 \pm 1.8$
2m	2-phenylethyl	4-nitrophenyl	$4.1 \times 10^4 \pm 1.1$
2n	4-fluorophenyl	4-nitrophenyl	$2.6 \times 10^3 \pm 1.5$
2o	4-chlorophenyl	4-nitrophenyl	$2.5 \times 10^3 \pm 1.1$
2p	4-nitrophenyl	4-nitrophenyl	$7.7 \times 10^5 \pm 1.2$

Mean ± SEM.

Table 4
The interaction of compounds with DNA.

Compound	R_1	R_2	Ksv (M^{-1})
1a	H	–	$9.0 \times 10^4 \pm 1.1$
1b	Allyl	–	$1.8 \times 10^3 \pm 1.1$
1c	phenyl	–	$1.6 \times 10^3 \pm 1.3$
1d	4-methylphenyl	–	$3.0 \times 10^4 \pm 1.0$
1e	4-ethylphenyl	–	$2.5 \times 10^3 \pm 1.9$
1f	4-methoxyphenyl	–	$9.0 \times 10^3 \pm 1.0$
1g	2-phenylethyl	–	$9.0 \times 10^4 \pm 0.0$
1h	4-fluorophenyl	–	$1.0 \times 10^2 \pm 1.1$
1i	4-chlorophenyl	–	$6.0 \times 10^4 \pm 1.2$
1j	4-bromophenyl	–	$1.4 \times 10^3 \pm 1.1$
1k	4-nitrophenyl	–	$1.3 \times 10^3 \pm 1.4$
1l	3-pyridyl	–	$1.8 \times 10^3 \pm 1.9$
1m	1-naphthyl	–	$3.4 \times 10^3 \pm 1.0$
2a	Allyl	phenyl	$9.0 \times 10^4 \pm 1.2$
2b	phenyl	phenyl	$3.8 \times 10^3 \pm 1.0$
2c	4-methylphenyl	phenyl	$2.3 \times 10^3 \pm 1.4$
2d	4-methoxyphenyl	phenyl	$1.1 \times 10^3 \pm 1.2$
2e	3-pyridyl	phenyl	$9.0 \times 10^4 \pm 1.7$
2f	1-naphthyl	phenyl	$2.5 \times 10^3 \pm 1.9$
2g	H	4-nitrophenyl	$2.0 \times 10^3 \pm 1.6$
2h	Allyl	4-nitrophenyl	$3.1 \times 10^3 \pm 1.3$
2i	phenyl	4-nitrophenyl	$1.7 \times 10^3 \pm 0.9$
2j	4-methylphenyl	4-nitrophenyl	$1.7 \times 10^3 \pm 0.7$
2k	4-ethylphenyl	4-nitrophenyl	$3.5 \times 10^3 \pm 1.1$
2l	4 methoxyphenyl	4-nitrophenyl	$3.9 \times 10^3 \pm 1.5$
2m	2-phenylethyl	4-nitrophenyl	$3.6 \times 10^3 \pm 1.1$
2n	4-fluorophenyl	4-nitrophenyl	$3.8 \times 10^3 \pm 1.3$
2o	4-chlorophenyl	4-nitrophenyl	$3.2 \times 10^3 \pm 1.9$
2p	4-nitrophenyl	4-nitrophenyl	$2.0 \times 10^3 \pm 1.3$

Mean ± SEM.

investigated the interaction of thiosemicarbazone and thiazole compounds against serum albumin and DNA. Silva Filho et al. (2019) found that acridine-thiosemicarbazone derivatives obtained Ksv values ranging from 3.46×10^2 to 7.83×10^3 M^{-1} for albumin, in addition to being capable of interacting with DNA.

Ribeiro et al. (2019) performed a binding study with DNA and BSA, they verified that all compounds showed an affinity for interaction with both biomolecules, especially JF-92 (p -substituted ethyl), with a binding constant of 1.62×10^6 and 1.43×10^5 M^{-1} respectively. Alves et al. (2021a) obtained interaction results of the compounds indole-thiazole and indole-thiazolidinone with albumin (Ksv), ranging from 0.79×10^4 to 4.34×10^4 M^{-1}. In another study Alves et al. (2021b) evaluating the interaction of indole-thiazole and indole-thiazolidinone compounds with DNA, obtained ksv values ranging from 0.38,10^4 to 7.59×10^4 M^{-1}. These findings affirm that the interaction between the evaluated macromolecules is directly related to the chemical structure.

3.4. Evaluation of cytotoxic activity against mammalian cells

The tests were performed with the aim of selecting the least toxic compounds against animal cells (RAW 264.7 macrophages, Chinese hamster lung fibroblasts (V79), hepatoma (HepG2), and erythrocytes). Table 5 presents the cytotoxicity results for all compounds obtained in this study.

Regarding the cytotoxicity studies, the results demonstrated CC_{50} values for RAW macrophages 264.7, values that ranged from 81.43 μM to values greater than 200 μM, for thiosemicarbazones-based analogues. While thiazoles exhibited CC_{50} values from 81.43 μM to values greater than 200 μM.

The CC_{50} for fibroblast cells (V79) ranged from 100.9 μM to values greater than 200 μM for thiosemicarbazones and for thiazoles it ranged from 100.21 μM to values greater than 200 μM.

For HepG2 cells, CC_{50} values ranged from 111.2 μM to values greater than 200 μM for thiosemicarbazones, and for thiazoles they ranged from 132.1 μM to values greater than 200 μM.

Table 5
In vitro cytotoxicity promoted by the synthesized compounds against RAW 264.7 macrophage cells, Chinese hamster lung fibroblasts (V79), hepatoma (HepG2) and erythrocytes respectively.

Compound	R1	R2	Macrophages (RAW 264.7) CC_{50} (μM)	Fibroblasts (V79) CC_{50} (μM)	Hepatoma (HepG2) CC_{50} (μM)	Hemolysis (%) Concentration (200–6 μM)
1a	H	–	>200	>200	>200	~5.0%
1b	Allyl	–	>200	>200	>200	~5.0%
1c	phenyl	–	81.43 ± 0.1	120.3 ± 1.1	154.8 ± 2.1	~5.0%
1d	4-methylphenyl	–	84.15 ± 0.3	100.9 ± 0.2	111.2 ± 0.1	~5.0%
1e	4-ethylphenyl	–	137.86 ± 0.5	>200	>200	~5.0%
1f	4-methoxyphenyl	–	139.04 ± 0.1	>200	>200	~5.0%
1g	2-phenylethyl	–	>200	>200	>200	~5.0%
1h	4-fluorophenyl	–	>200	>200	>200	~5.0%
1i	4-chlorophenyl	–	184.08 ± 0.0	190.5 ± 0.1	199.4 ± 0.2	~5.0%
1j	4-bromophenyl	–	>200	>200	>200	~5.0%
1k	4-nitrophenyl	–	93.23 ± 0.4	110.4 ± 0.1	132.8 ± 0.1	~5.0%
1l	3-pyridyl	–	>200	>200	>200	~5.0%
1m	1-naphthyl	–	>200	>200	>200	~5.0%
2a	Allyl	phenyl	>200	>200	>200	~5.0%
2b	Phenyl	phenyl	>200	>200	>200	~5.0%
2c	4-methylphenyl	phenyl	121.22 ± 0.3	143.2 ± 0.2	187.3 ± 0.9	~5.0%
2d	4-methoxyphenyl	phenyl	128.87 ± 0.6	167.3 ± 0.3	189.5 ± 0.2	~5.0%
2e	3-pyridyl	phenyl	127.70 ± 1.2	135.4 ± 1.1	190.3 ± 0.8	~5.0%
2f	1-naphthyl	phenyl	89.87 ± 0.2	100.21 ± 0.3	132.1 ± 0.1	~5.0%
2g	H	4-nitrophenyl	>200	>200	>200	~5.0%
2h	Allyl	4-nitrophenyl	>200	>200	>200	~5.0%
2i	phenyl	4-nitrophenyl	113.44 ± 0.1	124.3 ± 0.3	166.8 ± 1.4	~5.0%
2j	4-methylphenyl	4-nitrophenyl	>200	>200	>200	~5.0%
2k	4-ethylphenyl	4-nitrophenyl	>200	>200	>200	~5.0%
2l	4-methoxyphenyl	4-nitrophenyl	>200	>200	>200	~5.0%
2m	2-phenylethyl	4-nitrophenyl	>200	>200	>200	~5.0%
2n	4-fluorophenyl	4-nitrophenyl	198.96 ± 0.1	>200	>200	~5.0%
2o	4-chlorophenyl	4-nitrophenyl	>200	>200	>200	~5.0%
2p	4-nitrophenyl	4-nitrophenyl	>200	>200	>200	~5.0%
Miltefosine	–	–	7.1 ± 0.0	>200	150.90 ± 0.1	~5.0%
Amphotericin B	–	–	15.57 ± 0.2	>200	125.70 ± 1.1	~5.0%
Benznidazole	–	–	123.9 ± 0.7	>200	>200	~5.0%
Chloroquine	–	–	>200	>200	>200	~5.0%

Mean ± SEM.

Regarding the hemolytic assays, all compounds were not able to promote hemolysis since the values at all concentrations (200–6 μM) studied were less than 5%. These results affirm that thiazoles in general showed greater toxicity when compared to thiosemicarbazones.

The literature presents different results of *in vitro* cytotoxicity. Queiroz et al. (2020) investigating the cytotoxicity of 2 thiosemicarbazones (JW-16.2 and JW-37.2) and 2 thiazoles (GT-12 and GT-14) against peritoneal macrophages cells and obtained values ranging from 31.80 to 184.58 μM and 85.24–196.38 μM respectively. In addition, the authors obtained hemolysis percentages of approximately 5 and 4% for thiosemicarbazones and thiazoles, respectively. Santos-Silva et al. (2017) verifying the cytotoxicity of 2-pyridyl-2,3-thiazole derivatives against animal cells, obtained IC_{50} values greater than 50 μM for HepG2 cells and 250 μM for human erythrocytes. The results show that toxicity is directly related to the chemical structure and cell type evaluated.

3.5. *In vitro antiparasitic activity*

3.5.1. *Leishmanicidal and trypanocidal activity in vitro*

The selection of compounds was based on the adaptation of the scales proposed by Upegui et al. (2014) and Álvarez et al. (2017) where compounds that presented $IC_{50} < 50$ μM were considered active, those that presented IC_{50} between 50 and 150 μM moderately active and inactive with $IC_{50} > 150$ μM, against the different forms of the parasites. In addition, to this scale, it was possible to study the selectivity (through the selectivity index) and specificity (through the specificity index) of each compound against intracellular forms (Queiroz et al. 2020; Silva et al. 2020; Zuma et al. 2021). Therefore, to assess selectivity and specificity, scales were adapted from Lenta et al. (2007) and Don and Ioset (2014). That is, compounds that presented SI values > 1.0 indicate that they are more toxic to the parasite and those that presented SI values < 1.0 are more toxic to animal cells.

The specificity of the compound between the two forms of the parasite, promastigote or trypomastigote and amastigote, was determined by the specificity index (SPI) (Don and Ioset, 2014). Therefore, SPI values $>$ 1.0 indicate that the compound was more active for the amastigote forms. SPI values $<$ 0.7 suggest that the compound was more effective for the promastigote or trypomastigote forms. Compounds with IE values between 0.7 and 1.0 are considered active for the promastigote or trypomastigote and amastigote forms.

Tables 6 and 7 present the results of leishmanicidal and trypanocidal activity promoted by the compounds respectively. The results were expressed in terms of IC_{50}, selectivity index, and specificity.

The results presented in Table 6 show that thiosemicarbazones promoted IC_{50} ranging from 31.15 to 200 μM. The thiazoles presented values that ranged from 16.48 to 247.59 μM for the promastigote of *L. amazonensis* respectivement. In the amastigote form, the thiosemicarbazones presented IC_{50} values that ranged from 73.45 to 362.58 μM. The thiazoles showed values ranging from 50.80 to 379.25 μM respectively. Amastigote forms are found in the definitive host. Therefore, the most promising compounds for these forms of *L. amazonensis* in order of greater toxicity (IC_{50}) were: 2a $>$ 2l $>$ 2h $>$ 1j $>$ 1b.

Table 7 presents the results of the trypanocidal activity. The thiosemicarbazones presented IC_{50} values that ranged from 1.93 to 100 μM. The thiazoles presented values that varied from 7.20 to 100 μM for the trypomastigote forms. For the amastigote form, they presented values ranging from 5.54 to 292 μM for thiosemicarbazones and 8.08–250 μM for thiazoles. Through these results, we can select molecules 1b, 1j, and 2t that present dual activity, that is, they present promising results for *L. amazonensis* as for *T. cruzi*.

The literature presents different compounds that show potential against these parasites. Castro Levatti et al. (2022) evaluated licarin A derivatives containing o-allyl (1b) and 5-allyl (1c) substituents, they obtained IC_{50} of 24.2 and 9.9 μM for the promastigote forms and 13.2 and 10.8 μM for the amastigote forms of Leishmania Infantum, respectively. Barbosa et al. (2009) found that compound 4 with 4-bromophenyl substituent promoted the highest cytotoxic activity against promastigote forms of Leishmania Infantum with an IC_{50} of 25.2 μM.

Kaplum et al. (2016) verified that the compound LPSN331, which presents the 4-methoxyphenyl group, presented an IC_{50} of 30 μM for the promastigote form and 19.3 μM for the amastigote forms, respectively. Espíndola et al. (2015) evaluated the effect of different aryloxyl thiosemicarbazones, they obtained IC_{50} values ranging from 1.8 to 15.7 μM for the epimastigote forms and 1.6–15.6 μM for the trypomastigote forms. These results show that the allyl, 4-bromophenyl and 4-methoxyphenyl substituents have substituents with leishmanicidal and trypanocidal potential.

3.5.2. Anti - *P. falciparum* activity in vitro

The compounds were assessed against 3D7 strains of *P. falciparum*, the cytotoxicity results were evaluated through the IC_{50}. The activity results are shown in Table 8.

The thiosemicarbazones were not able to inhibit the growth of *P. falciparum* parasites. In contrast, thiazoles were able to promote growth inhibition with IC_{50} results ranging from 0.47 to 4.11 μM except compounds 2g, 2l, and 2p which did not promote growth inhibition. Among the compounds evaluated in this activity, 4 showed promising results. These were arranged in order of greatest toxicity 2h $>$ 2f $>$ 2k $>$ 2j.

Compounds 2h, 2j and 2k contain the 4-nitrophenyl substitution at C-4. The nitro group is well known for its important contribution to molecules with an antiparasitic profile, hence its choice as a surrogate group in the molecules of this study (Paulai et al., 2009). The allyl group (2p MlogP = 4.08) in N-3 promoted an excellent result with IC_{50} = 0.47 μM, being the most active compound among all thiazoles. Lipophilicity (logP) is considered the most important physicochemical property for the drug discovery and development process. Scarim et al. (2019) in their review showed that the best antimalarial compounds had a logP value ranging from 3.31 to 4.42. These data in association with the presence of the 4-nitrophenyl group at C-4 may have contributed to the activity.

Table 6
Leishmanicidal activity against the promastigote and amastigote forms of *L. amazonensis*.

Compound	R_1	R_2	*L. amazonensis*		Selectivity Indices	Specificity Indices
			Promastigote IC_{50} (μM)	Amastigote IC_{50} (μM)	Amastigote CC_{50}/IC_{50}	IC_{50}/IC_{50}
1a	H	–	200.0 ± 0.1	362.58 ± 1.3	>0.55	0.55
1b	Allyl	–	21.56 ± 0.01	96.6 ± 0.1	>2.07	0.22
1c	phenyl	–	200.0 ± 0.1	263.91 ± 0.1	0.31	0.76
1d	4-methylphenyl	–	200.0 ± 0.2	132.42 ± 0.12	0.64	1.51
1e	4-ethylphenyl	–	200.0 ± 0.3	84.87 ± 1.2	1.62	2.36
1f	4-methoxyphenyl	–	200.0 ± 1.0	318.40 ± 1.1	0.44	0.63
1g	2-phenylethyl	–	31.15 ± 0.01	100 ± 0.2	>2.00	0.31
1h	4-fluorophenyl	–	200.0 ± 0.1	330.25 ± 1.0	>0.61	0.61
1i	4-chlorophenyl	–	57.11 ± 0.01	124.46 ± 0.02	1.48	0.46
1j	4-bromophenyl	–	200.0 ± 0.12	73.45 ± 0.01	>2.72	2.72
1k	4-nitrophenyl	–	200.0 ± 1.0	100.0 ± 0.5	0.93	2.00
1l	3-pyridyl	–	200.0 ± 0.3	131.24 ± 0.9	>1.52	1.52
1m	1-naphthyl	–	37.02 ± 0.1	100.0 ± 0.1	>2.00	0.37
2a	Allyl	phenyl	57.62 ± 0.2	50.80 ± 0.2	>3.94	1.13
2b	phenyl	phenyl	200.0 ± 0.1	201.0 ± 0.9	>1.00	1.00
2c	4-methylphenyl	phenyl	77.13 ± 0.2	205 ± 0.1	0.59	0.38
2d	4-methoxyphenyl	phenyl	200 ± 0.1	244.98 ± 0.3	0.53	0.82
2e	3-pyridyl	phenyl	16.48 ± 0.4	210.0 ± 0.3	0.61	0.08
2f	1-naphthyl	phenyl	92.87 ± 0.1	102.1 ± 0.2	0.88	0.91
2g	H	4-nitrophenyl	221.64 ± 0.0	379.25 ± 0.1	>0.53	0.58
2h	Allyl	4-nitrophenyl	200.0 ± 0.3	66.46 ± 0.2	>3.01	3.01
2i	phenyl	4-nitrophenyl	200.0 ± 0.3	178.90 ± 0.2	0.63	1.12
2j	4-methylphenyl	4-nitrophenyl	200.0 ± 0.1	264.77 ± 0.3	>0.76	0.76
2k	4-ethylphenyl	4-nitrophenyl	200.0 ± 0.1	100.0 ± 0.3	>2.00	2.00
2l	4-methoxyphenyl	4-nitrophenyl	200.0 ± 0.9	66.13 ± 0.1	>3.02	3.02
2m	2-phenylethyl	4-nitrophenyl	200.0 ± 0.2	204.0 ± 0.2	>0.98	0.98
2n	4-fluorophenyl	4-nitrophenyl	247.59 ± 0.1	100.0 ± 0.1	1.99	2.48
2o	4-chlorophenyl	4-nitrophenyl	200.0 ± 0.9	100.0 ± 0.4	>2.00	2.00
2p	4-nitrophenyl	4-nitrophenyl	200.0 ± 0.1	72.69 ± 0.1	>2.75	2.75
Miltefosine	–	–	0.13 ± 0.01	7.75 ± 0.01	0.91	0.01
Amphotericin B	–	–	15.83 ± 0.01	8.97 ± 0.02	1.73	1.76

Mean ± SEM.

Table 7
Trypanocidal activity against the trypomastigote and amastigote forms of *T. cruzi.*

Compound	R_1	R_2	T. *cruzi*		Selectivity Indices	Specificity Indices
			Trypomastigote IC_{50} (μM)	Amastigote IC_{50} (μM)	Amastigote CC_{50}/IC_{50}	IC_{50}/IC_{50}
1a	H	–	60.18 ± 0.2	88.24 ± 0.2	>2.27	0.68
1b	Allyl	–	1.93 ± 0.01	5.54 ± 0.02	>36.10	0.35
1c	phenyl	–	9.29 ± 0.022	211.1 ± 1.0	0.39	0.04
1d	4-methylphenyl	–	100.1 ± 0.1	222.2 ± 0.3	0.38	0.45
1e	4-ethylphenyl	–	17.51 ± 0.04	248.2 ± 0.01	0.56	0.07
1f	4-methoxyphenyl	–	100.0 ± 0.01	292.0 ± 1.0	0.48	0.34
1g	2-phenylethyl	–	10.16 ± 0.01	7.88 ± 0.02	>25.38	1.29
1h	4-fluorophenyl	–	100.01 ± 0.2	61.84 ± 0.01	>3.23	1.62
1i	4-chlorophenyl	–	58.38 ± 0.10	41.72 ± 0.1	4.41	1.40
1j	4-bromophenyl	–	27.06 ± 0.12	52.03 ± 0.11	>3.84	0.52
1k	4-nitrophenyl	–	100.0 ± 0.1	211.0 ± 0.2	0.44	0.47
1l	3-pyridyl	–	3.80 ± 0.01	9.82 ± 0.00	>20.37	0.39
1m	1-naphthyl	–	2.25 ± 0.02	3.82 ± 0.01	>52.36	0.59
2a	Allyl	phenyl	100.0 ± 0.1	235.0 ± 1.0	>0.85	0.43
2b	phenyl	phenyl	100.0 ± 0.2	250.0 ± 0.1	>0.80	0.40
2c	4-methylphenyl	phenyl	100.0 ± 0.1	212.0 ± 0.3	0.57	0.47
2d	4-methoxyphenyl	phenyl	100.0 ± 0.9	214.1 ± 0.2	0.60	0.47
2e	3-pyridyl	phenyl	7.20 ± 0.01	8.08 ± 0.02	15.80	0.89
2f	1-naphthyl	phenyl	100.0 ± 0.02	201.0 ± 0.3	0.45	0.50
2g	H	4-nitrophenyl	56.06 ± 0.1	80.01 ± 1.1	>2.50	0.70
2h	Allyl	4-nitrophenyl	100.0 ± 0.2	209.0 ± 0.1	>0.96	0.48
2i	phenyl	4-nitrophenyl	100.0 ± 0.1	202.0 ± 1.1	0.56	0.50
2j	4-methylphenyl	4-nitrophenyl	100.0 ± 0.4	205.0 ± 1.9	>0.98	0.49
2k	4-ethylphenyl	4-nitrophenyl	100.0 ± 0.1	208.0 ± 0.9	>0.96	0.48
2l	4-methoxyphenyl	4-nitrophenyl	13.11 ± 0.1	16.43 ± 0.1	>12.17	0.80
2m	2-phenylethyl	4-nitrophenyl	100.0 ± 0.2	210.1 ± 0.3	>0.95	0.48
2n	4-fluorophenyl	4-nitrophenyl	100.0 ± 0.9	206.2 ± 0.2	0.97	0.49
2o	4-chlorophenyl	4-nitrophenyl	100.0 ± 1.0	201.1 ± 1.1	>1.00	0.50
2p	4-nitrophenyl	4-nitrophenyl	100.0 ± 1.1	220.1 ± 1.2	>0.91	0.45
Benznidazole	–	–	14.60 ± 0.2	5.65 ± 0.02	21.87	2.58

Mean ± SEM.

Table 8
Cytotoxicity promoted by the compounds against *P. falciparum in vitro.*

Compound	R_1	R_2	*P. falciparum* IC_{50} (μM)
1a	H	–	-
1b	Allyl	–	-
1c	phenyl	–	-
1d	4-methylphenyl	–	-
1e	4-ethylphenyl	–	-
1f	4-methoxyphenyl	–	-
1g	2-phenylethyl	–	-
1h	4-fluorophenyl	–	-
1i	4-chlorophenyl	–	-
1j	4-bromophenyl	–	-
1k	4-nitrophenyl	–	-
1l	3-pyridyl	–	-
1m	1-naphthyl	–	-
2a	Allyl	phenyl	2.05 ± 0.01
2b	phenyl	phenyl	2.91 ± 0.02
2c	4-methylphenyl	phenyl	2.29 ± 0.01
2d	4-methoxyphenyl	phenyl	1.54 ± 0.08
2e	3-pyridyl	phenyl	4.11 ± 0.01
2f	1-naphthyl	phenyl	0.53 ± 0.02
2g	H	4-nitrophenyl	–
2h	Allyl	4-nitrophenyl	0.47 ± 0.01
2i	phenyl	4-nitrophenyl	2.67 ± 0.01
2j	4-methylphenyl	4-nitrophenyl	0.79 ± 0.0
2k	4-ethylphenyl	4-nitrophenyl	0.69 ± 0.03
2l	4 methoxyphenyl	4-nitrophenyl	–
2m	2-phenylethyl	4-nitrophenyl	1.48 ± 0.02
2n	4-fluorophenyl	4-nitrophenyl	–
2o	4-chlorophenyl	4-nitrophenyl	1.51 ± 0.01
2p	4-nitrophenyl	4-nitrophenyl	–
Chloroquine	–	–	0.075 ± 0.0

Mean ± SEM.

Nitrocompounds are correlated with antiparasitic activity due to the generation of reactive oxygen species (ROS) that alter redox processes leading to increased oxidative stress. ROS attack enzymes, affect the cell membrane and promote DNA damage that justifies their mode of action. The replacement of hydrogen in N-3 by a phenyl group (compound 2i) showed $IC_{50} = 2.67$ μM. When the phenyl group is replaced by 4-methyl (compound 2j) and 4-ethyl (compound 2k) groups, an increase in biological activity occurs, represented by the values of $IC_{50} = 0.79$ μM and $IC_{50} = 0.69$ μM, respectively, confirming the importance of the alkyl groups attached to the phenyl group.

The literature reveals the existence of a halogen bond that consists of a non-covalent interaction between halogen and another electronegative atom and is of great importance in the formation of the ligand-protein complex (Gutiérrez et al. 2016). Next, the influence of halogens on antimalarial activity was investigated, since the presence of these atoms usually leads to an increase in drug absorption (Gerebtzoff et al. 2004) and facilitates their crossing through the blood-brain barrier (Gentry et al. 1999), a fundamental aspect for the treatment of the severe cerebral form of malaria (WHO, 2020). Thus, the 4-chlorophenyl group for the R2 portion of the thiazole ring bearing the 4-nitro group at N-3 was selected. This compound showed $IC_{50} = 0.79$ μM. This proves, once again, the importance of the $–NO_2$ group and the halogen (chlorine) for antiparasitic activity.

A very interesting result was obtained when the same phenyl group was replaced by the 1-naphthyl group (compound 2f) with a significant increase in antimalarial activity with $IC_{50} = 0.53$ μM. The presence of the naphthyl group in molecules with antiparasitic activity has been widely studied (Verhaeghe et al. 2009; Heinrich et al. 2011; Cohen et al. 2012). Balabadra et al. (2017) suggested that the bioisosteric substitution of quinoline by the naphthalene group is important in their compounds, since the presence of the naphthyl group is associated with a strong π-π interaction with hydrophobic residues of biological targets of *P. falciparum*.

4. Conclusion

The results of the *in silico* study (ADME) showed that the compounds have potential oral availability, according lipinski and veber rules. In albumin interaction assays the compounds showed interactions that ranged from low to high. In relation to DNA interaction assays, the compounds showed moderate to low interaction. Besides that, all these compounds (1a - m; 2a - p) exhibited promising antioxidant effects. Cytotoxicity assays against animal cells revealed that thiosemicarbazones (1a – 1m) were less toxic when compared to thiazoles (2a – p). In antiparasitic activity assays, the compounds showed promise against different forms of *L. amazonensis* and *T. cruzi*. Finally, in cytotoxicity assays against the *P. falciparum* strain, only thiazoles were able to inhibit the growth of the parasite *in vitro*. Therefore, this study showed that the compounds evaluated here can be classified as possible drug candidates against different parasites *in vitro*.

CRediT author statement

Natali de França Nibbering Santos: Conceptualization, Investigation, Methodology, Validation, Formal analysis, Writing - Original Draft, Writing - Review & Editing; **Natanael da Silva Bezerra Junior:** Conceptualization, Investigation, Methodology, Validation, Formal analysis, Writing - Original Draft, Writing - Review & Editing; **Jamerson Ferreira de Oliveira:** Conceptualization, Investigation, Methodology, Validation, Formal analysis, Writing - Original Draft, Writing - Review & Editing: **Denise Maria Figueiredo Araújo Duarte:** Conceptualization, Investigation, Methodology, Validation, Formal analysis, Writing - Original Draft, Writing - Review & Editing; **Diego Santa Clara Marques:** Conceptualization, Investigation, Methodology, Validation, Formal analysis, Writing - Original Draft, Writing - Review & Editing; **José Cleberson dos santos Soares:** Conceptualization, Investigation, Methodology, Validation, Formal analysis, Writing - Original Draft, Writing - Review & Editing; **Aline Caroline da Silva Santos:** Conceptualization, Investigation, Methodology, Validation, Formal analysis, Writing - Original Draft, Writing - Review & Editing: **Fátima Nogueira:** Conceptualization, Investigation, Methodology, Validation, Formal analysis, Writing - Original Draft, Writing - Review & Editing; **Valéria Rêgo Alves Pereira:** Conceptualization, Investigation, Methodology, Validation, Formal analysis, Writing - Original Draft, Writing - Review & Editing; **Maria do Carmo Alves de Lima:** Conceptualization, Methodology, Formal analysis, Resources, Writing - Original Draft, Writing - Review & Editing, Supervision, Project administration; **Iranildo José da Cruz Filho:** Conceptualization, Methodology, Formal analysis, Resources, Writing - Original Draft, Writing - Review & Editing, Supervision, Project administration.

Declaration of competing interest

The authors declare that they have no known competing financial interests or personal relationships that could have appeared to influence the work reported in this paper.

Data availability

Data will be made available on request.

Acknowledgment

This study was funded by Brazilian agencies Research Support Foundation of the State of Pernambuco - FACEPE (Process APQ-0498-4.03/19), Research Fellowship - FACEPE (Process BFP-0038-04.03/21) and National Council for Scientific and Technological Development - CNPq (Process 306865/612020–3). In addition to these, we also thank the Nucleus of Analysis and Research in Nuclear Magnetic Resonance (NAPRMN) - Federal University of Alagoas for all spectrum acquisition. Thanks to MR4, who provided us with thePlasmodium falciparum MRA-1029 strain provided by Andrew Talman, Robert Sinden that we used in the assays. The work was partially supported by FCT project reference CIRCNA/BRB/0281/2019_AMAZING and GHTM-UID/Multi/04413/2013.

Appendix A. Supplementary data

Supplementary data to this article can be found online at https://doi.org/10.1016/j.exppara.2023.108498.

References

Achan, J., Mwesigwa, J., Edwin, C.P., D'alessandro, U., 2018. Malaria medicines to address drug resistance and support malaria elimination efforts. Expet Rev. Clin. Pharmacol. 11 (1), 61–70.

Ali, S.H., Sayed, A.R., 2021. Review of the synthesis and biological activity of thiazoles. Synth. Commun. 51 (5), 670–700. https://doi.org/10.1080/00397911.2020.1854787.

Álvarez, G., Perdomo, C., Coronel, C., Aguilera, E., Varela, J., Aparicio, G., et al., 2017. Multi-anti-parasitic activity of arylidene ketones and thiazolidene hydrazines against Trypanosoma cruzi and Leishmania spp. Molecules 22 (5), 709. https://doi.org/10.3390/molecules22050709.

Alves, J.E.F., Lucena, M.L.C., Souza Lucena, A.E., Merces, A.A.D., Azevedo, R.D.S., Sousa, G.L.S., et al., 2021a. A simple method for obtaining human albumin and its use for in vitro interaction assays with indole-thiazole and indole-thiazolidinone derivatives. Int. J. Biol. Macromol. 192, 126–137. https://doi.org/10.1016/j.ijbiomac.2021.09.109.

Alves, J.E.F., Oliveira, J.F., Lima Souza, T.R.C., Moura, R.O., Carvalho Junior, L.B., de Lima, M.D.C.A., Almeida, S.M.V., 2021b. Novel indole-thiazole and indole-thiazolidinone derivatives as DNA groove binders. Int. J. Biol. Macromol. 170, 622–635. https://doi.org/10.1016/j.ijbiomac.2020.12.153.

Amin, K., Dannenfelser, R.M., 2006. In vitro hemolysis: guidance for the pharmaceutical scientist. J. Pharmaceut. Sci. 95 (6), 1173–1176. https://doi.org/10.1002/jps.20627.

Araújo Neto, L.N., Lima, M.D.C.A., de Oliveira, J.F., Souza, E.R., Buonafina, M.D.S., Anjos, M.N.V., Mendonça-Junior, F.J.B., 2017. Synthesis, cytotoxicity and antifungal activity of 5-nitro-thiophene-thiosemicarbazones derivatives. Chem. Biol. Interact. 272, 172–181. https://doi.org/10.1016/j.cbi.2017.05.005.

Balabadra, S., Kotni, M., Manga, V., Allanki, A.D., Prasad, R., Sijwali, P.S., 2017. Synthesis and evaluation of naphthyl bearing 1,2,3-Triazole analogs as antiplasmodial agents, cytotoxicity and docking studies. Bioorg. Med. Chem. 25 (2017), 221–232. https://doi.org/10.1016/j.bmc.2016.10.029.

Barbosa, T.P., Junior, C.G., Silva, F.P., Lopes, H.M., Figueiredo, L.R., Sousa, S.C., Vasconcellos, M.L., 2009. Improved synthesis of seven aromatic Baylis–Hillman adducts (BHA): evaluation against Artemia salina Leach. and Leishmania chagasi. Eur. J. Med. Chem. 44 (4), 1726–1730. https://doi.org/10.1016/j.ejmech.2008.03.016.

Castro Levatti, E.V., Costa-Silva, T.A., Morais, T.R., Fernandes, J.P.S., Lago, J.H.G., Tempone, A.G., 2022. Natural product-based drug discovery: mechanistic studies of licarin a derivatives on Leishmania (L.) infantum. Available at SSRN: https://ssrn.com/abstract=4066149 https://doi.org/10.2139/ssrn.4066149.

Chattopadhyay, A., Jafurulla, M., 2011. A novel mechanism for an old drug: amphotericin B in the treatment of visceral leishmaniasis. Biochem. Biophys. Res. Commun. 416 (1–2), 7–12. https://doi.org/10.1016/j.bbrc.2011.11.023.

Chen, X., Li, H., Tian, L., Li, Q., Luo, J., Zhang, Y., 2020. Analysis of the physicochemical properties of acaricides based on Lipinski's rule of five. J. Comput. Biol. 27 (9), 1397–1406. https://doi.org/10.1089/cmb.2019.0323.

Cohen, A., Verhaeghe, P., Crozet, M.D., Hutter, S., Rathelot, P., Vanelle, P., Azas, N., 2012. Tandem synthesis and in vitro antiplasmodial evaluation of new naphtho[2,1-d]thiazole derivatives. Eur. J. Med. Chem. 55 (2012), 315–324. https://doi.org/10.1016/j.ejmech.2012.07.034.

Daina, A., Michielin, O., Zoete, V., 2017. SwissADME: a free web tool to evaluate pharmacokinetics, drug-likeness and medicinal chemistry friendliness of small molecules. Sci. Rep. 7 (1), 1–13. https://doi.org/10.1038/srep42717.

Don, R.O.B., Ioset, J.R., 2014. Screening strategies to identify new chemical diversity for drug development to treat kinetoplastid infections. Parasitology 141 (1), 140–146. https://doi.org/10.1017/S003118201300142X.

Du, X., Guo, C., Hansell, E., Doyle, P.S., Caffrey, C.R., Holler, T.P., et al., 2002. Synthesis and structure– activity relationship study of potent trypanocidal thio semicarbazone inhibitors of the trypanosomal cysteine protease cruzain. J. Med. Chem. 45 (13), 2695–2707. https://doi.org/10.1021/jm010459j.

Espíndola, J.W.P., de Oliveira Cardoso, de Oliveira Filho, e Silva, Moreira, D.R.M., Bastos, T.M., Leite, A.C.L., 2015. Synthesis and structure–activity relationship study of a new series of antiparasitic aryloxyl thiosemicarbazones inhibiting Trypanosoma Cruzi Cruzain. Eur. J. Med. Chem. 101, 818–835. https://doi.org/10.1016/j.ejmech.2015.06.048.

Freitas, L.A.B., Silva Santos, A.C., Cássia Silva, G., Nascimento Albuquerque, F.N., Silva, E.D., Simone, C.A., Moraes Gomes, P.A.T., 2021. Structural improvement of new thiazolyl-isatin derivatives produces potent and selective trypanocidal and leishmanicidal compounds. Chem. Biol. Interact. 345, 109561 https://doi.org/10.1016/j.cbi.2021.109561.

García-Huertas, P., Cardona-Castro, N., 2021. Advances in the treatment of Chagas disease: promising new drugs, plants and targets. Biomed. Pharmacother. 142, 112020 https://doi.org/10.1016/j.biopha.2021.112020.

Gentry, C.L., Egleton, R.D., Gillespie, T., Abbruscato, T.J., Bechowski, H.B., Hruby, V.J., Davis, T.P., 1999. The effect of halogenation on blood–brain barrier permeability of a novel peptide drug. Peptides 20, 1229–1238. https://doi.org/10.1016/s0196-9781(99)00127-8.

Gerebtzoff, G., Li-Blatter, X., Fischer, H., Frentzel, A., Seelig, 2004. Seelig, Halogenation of drugs enhances membrane binding and permeation. Chembiochem 5, 676–684. https://doi.org/10.1002/cbic.200400017.

Gouveia, A.L., Santos, F.A., Alves, L.C., Cruz-Filho, I.J., Silva, P.R., Jacob, I.T., Maria do Carmo, A.L., 2022. Thiazolidine derivatives: in vitro toxicity assessment against promastigote and amastigote forms of Leishmania infantum and ultrastructural study. Exp. Parasitol. 236, 108253 https://doi.org/10.1016/j.exppara.2022.108253.

Gutiérrez, I.S., Lin, F.Y., Vanommeslaeghe, K., Lemkul, J.A., Armacost, K.A., Brooks III, C.L., MacKerell Jr., A.D., 2016. Parametrization of halogen bonds in the CHARMM general force field: improved treatment of ligand–protein interaction. Bioorg. Med. Chem. 24, 4812–4825. https://doi.org/10.1016/j.bmc.2016.06.034.

Heinrich, S., Altenkämper, M., Bechem, B., Perruchon, J., Ortmann, R., Dahse, H.M., Schlitzer, M., 2011. 2-Acylamino-5-chlorobenzophenones with enhanced selectivity towards malaria parasites. Eur. J. Med. Chem. 46, 1331–1342. https://doi.org/10.1016/j.ejmech.2011.01.056.

Jacob, Í.T., Gomes, F.O., Miranda, M.D., Almeida, S., Cruz-Filho, I.J., Peixoto, C.A., et al., 2021. Anti-inflammatory activity of novel thiosemicarbazone compounds indole-based as COX inhibitors. Pharmacol. Rep. 73 (3), 907–925. https://doi.org/10.1007/s43440-021-00221-7.

Jadhav, P.M., Kantevari, S., Tekale, A.B., Bhosale, S.V., Pawar, R.P., Tekale, S.U., 2021. A review on biological and medicinal significance of thiazoles. Phosphorus Sulfur Silicon Relat. Elements 196 (10), 879–895. https://doi.org/10.1080/10426507.2021.1945601.

Jaishree, V., Ramdas, N., Sachin, J., Ramesh, B., 2012. In vitro antioxidant properties of new thiazole derivatives. J. Saudi Chem. Soc. 16 (4), 371–376. https://doi.org/10.1016/j.jscs.2011.02.007.

Kanso, F., Khalil, A., Noureddine, H., El-Makhour, Y., 2021. Therapeutic perspective of thiosemicarbazones derivatives in inflammatory pathologies: a summary of in vitro/in vivo studies. Int. Immunopharm. 96, 107778 https://doi.org/10.1016/j.intimp.2021.107778.

Kaplancıklı, Z.A., Altıntop, M.D., Sever, B., Cantürk, Z., Özdemir, A., 2016. Synthesis and in vitro evaluation of new thiosemicarbazone derivatives as potential antimicrobial agents. J. Chem. 2016 https://doi.org/10.1155/2016/1692540.

Kaplum, V., Cogo, J., Sangi, D.P., Ueda-Nakamura, T., Corrêa, A.G., Nakamura, C.V., 2016. In vitro and in vivo activities of 2, 3-diarylsubstituted quinoxaline derivatives against Leishmania amazonensis. Antimicrob. Agents Chemother. 60 (6), 3433–3444. https://doi.org/10.1128/AAC.02582-15.

Lenta, B.N., Vonthron-Sénécheau, C., Soh, R.F., Tantangmo, F., Ngouela, S., Kaiser, M., Weniger, B., 2007. In vitro antiprotozoal activities and cytotoxicity of some selected Cameroonian medicinal plants. J. Ethnopharmacol. 111, 8–12. https://doi.org/10.1016/j.jep.2006.10.036.

Lipinski, C.A., Lombardo, F., Dominy, B.W., Feeney, P.J., 1997a. Experimental and computational approaches to estimate solubility and permeability in drug discovery and development settings. Adv. Drug Deliv. Rev. 23 (1–3), 3–25. https://doi.org/10.1016/s0169-409x(00)00129-0.

Lipinski, C.A., Lombardo, F., Dominy, B.W., Feeney, P.J., 1997b. Experimental and computational approaches to estimate solubility and permeability in drug discovery and development settings. Adv. Drug Deliv. Rev. 23 (1–3), 3–25. https://doi.org/10.1016/S0169-409X(96)00423-1.

Matsa, R., Makam, P., Kaushik, M., Hoti, S.L., Kannan, T., 2019. Thiosemicarbazone derivatives: design, synthesis and in vitro antimalarial activity studies. Eur. J. Pharmaceut. Sci. 137, 104986 https://doi.org/10.1016/j.bmc.2017.05.056, 10.1016/j.ejps.2019.104986.

Mic, M., Pîrnău, A., Floare, C.G., Marc, G., Franchini, A.H., Oniga, O., et al., 2021. Synthesis and molecular interaction study of a diphenolic hidrazinyl-thiazole compound with strong antioxidant and antiradical activity with HSA. J. Mol. Struct. 1244, 131278 https://doi.org/10.1016/j.molstruc.2021.131278.

Mishra, S., Bharti, P.K., Shukla, M.M., Ali, N.A., Kashyotia, S.S., Kumar, A., et al., 2017. Clinical and molecular monitoring of Plasmodium falciparum resistance to antimalarial drug (artesunate+ sulphadoxine-pyrimethamine) in two highly malarious district of Madhya Pradesh, central India from 2012–2014. Pathog. Glob. Health 111 (4), 186–194. https://doi.org/10.1080/20477724.2017.1331875.

Moraes Gomes, P.A.T., Oliveira Barbosa, M., Santiago, E.F., de Oliveira Cardoso, M.V., Costa, N.T.C., Hernandes, M.Z., et al., 2016. New 1, 3-thiazole derivatives and their biological and ultrastructural effects on Trypanosoma cruzi. Eur. J. Med. Chem. 121, 387–398.

Nam, S.Y., Han, N.R., Yoon, K.W., Kim, H.M., Jeong, H.J., 2017. Di-2-pyridylketone 4, 4-dimethyl-3-thiosemicarbazone (Dp44mT), an anticancer agent, exerts an anti-inflammatory effect in activated human mast cells. Inflamm. Res. 66 (10), 871–879. https://doi.org/10.1007/s00011-017-1067-x.

Oliveira, J.F., Nonato, F.R., Zafred, R.R.T., Leite, N.M.S., Ruiz, A.L.T.G., Carvalho, J.E., et al., 2016. Evaluation of anti-inflammatory effect of derivative (E)-N-(4-bromophenyl)-2-(thiophen-2-ylmethylene)-thiosemicarbazone. Biomed. Pharmacother. 80, 388–392. https://doi.org/10.1016/j.biopha.2016.03.047.

Paulai, F.R., Serrano, S.H.P., Tavares, L.C., 2009. Aspects of bioactivity and toxicity of nitrocompounds. Química Nova 32, 1013–1020. https://doi.org/10.1590/S0100-40422009000400032.

Pires, D.E., Blundell, T.L., Ascher, D.B., 2015. pkCSM: predicting small-molecule pharmacokinetic and toxicity properties using graph-based signatures. J. Med. Chem. 58 (9), 4066–4072. https://doi.org/10.1021/acs.jmedchem.5b00104.

Queiroz, C.M., Oliveira Filho, G.B., Espíndola, J.W.P., Nascimento, A.V., Aliança, A.S.D.S., Lorena, V.M.B., Brayner, F.A., 2020. Thiosemicarbazone and thiazole: in vitro evaluation of leishmanicidal and ultrastructural activity on Leishmania infantum. Med. Chem. Res. 29 (11), 2050–2065. https://doi.org/10.1007/s00044-020-02619-z.

Raevsky, O.A., Raevskaja, O.E., Schaper, K.J., 2004. Analysis of water solubility data on the basis of HYBOT descriptors. Part 3. Solubility of solid neutral chemicals and drugs. QSAR Comb. Sci. 23 (5), 327–343. https://doi.org/10.1002/qsar.200430862.

Ramsay, A., Olliaro, P., Reeder, J.C., 2016. The need for operational research and capacity-building in support of the Global Technical Strategy for Malaria 2016–2030. Malar. J. 15 (1), 1–3. https://doi.org/10.1186/s12936-016-1302-x.

Ribeiro, A.G., Almeida, S.M.V., Oliveira, J.F., Lima Souza, T.R.C., Santos, K.L., Barros Albuquerque, A.P., et al., 2019. Novel 4-quinoline-thiosemicarbazone derivatives: synthesis, antiproliferative activity, in vitro and in silico biomacromolecule interaction studies and topoisomerase inhibition. Eur. J. Med. Chem. 182, 111592 https://doi.org/10.1016/j.ejmech.2019.111592.

Ribeiro, A.G., Alves, J.E.F., Soares, J.C.S., Santos, K.L., Jacob, Í.T.T., Silva Ferreira, C.J., et al., 2021. Albumin roles in developing anticancer compounds. Med. Chem. Res. 30 (8), 1469–1495. https://doi.org/10.1007/s00044-021-02748-z.

Ruiz-Postigo, J.A., Jain, S., Mikhailov, A., Maia-Elkhoury, A.N., Valadas, S., Warusavithana, S., et al., 2021. Global leishmaniasis surveillance: 2019-2020, a baseline for the 2030 roadmap/Surveillance mondiale de la leishmaniose: 2019-2020, une periode de reference pour la feuille de route a l'horizon 2030. Wkly. Epidemiol. Rec. 96 (35), 401–420.

Salar, U., Khan, K.M., Chigurupati, S., Syed, S., Vijayabalan, S., Wadood, A., et al., 2019. New hybrid scaffolds based on hydrazinyl thiazole substituted coumarin; as novel leads of dual potential; in vitro α-amylase inhibitory and antioxidant (DPPH and ABTS radical scavenging) activities. Med. Chem. 15 (1), 87–101. https://doi.org/10.2174/1573406414666180903162243.

Santacruz, M.C.S., Fabiani, M., Castro, E.F., Cavallaro, L.V., Finkielsztein, L.M., 2017. Synthesis, antiviral evaluation and molecular docking studies of N4-aryl substituted/unsubstituted thiosemicarbazones derived from 1-indanones as potent anti-bovine viral diarrhea virus agents. Bioorg. Med. Chem. 25 (15), 4055–4063.

Santos, S.A., Lukens, A.K., Coelho, L., Nogueira, F., Wirth, D.F., Mazitschek, R., et al., 2015. Exploring the 3-piperidin-4-yl-1H-indole scaffold as a novel antimalarial chemotype. Eur. J. Med. Chem. 102, 320–333. https://doi.org/10.1016/j.ejmech.2015.07.047.

Santos Silva, T.D., Bomfim, L.M., Cruz Rodrigues, A.C.B., Dias, R.B., Sales, C.B.S., Rocha, C.A.G., Militão, G.C.G., 2017. Anti-liver cancer activity in vitro and in vivo induced by 2-pyridyl 2, 3-thiazole derivatives. Toxicol. Appl. Pharmacol. 329, 212–223. https://doi.org/10.1016/j.taap.2017.06.003.

Santos Silva, V.N., Santos, A.C.D.S., Pereira, V.R.A., Castro, M.C.A.B., 2021. Considerations about leishmaniasis and the current scenario for the development of new treatments. J. Trop. Pathol. 50 (4) https://doi.org/10.5216/rpt.v50i4.69817.

Scarim, C.B., Jornada, D.H., Machado, M.G.M., Ferreira, C.M.R., Dos Santos, J.L., Chung, M.C., 2019. Thiazole, thio and semicarbazone derivatives against tropical infective diseases: chagas disease, human African trypanosomiasis (HAT), leishmaniasis, and malaria. Eur. J. Med. Chem. 162, 378–395. https://doi.org/10.1016/j.ejmech.2018.11.013.

Scariot, D.B., Britta, E.A., Moreira, A.L., Falzirolli, H., Silva, C.C., Ueda-Nakamura, T., et al., 2017. Induction of early autophagic process on Leishmania amazonensis by synergistic effect of miltefosine and innovative semi-synthetic thiosemicarbazone. Front. Microbiol. 8, 255. https://doi.org/10.3389/fmicb.2017.00255.

Silva Filho, F.A., Souza, T.F., Ribeiro, A.G., Alves, J.E.F., Oliveira, J.F., Souza, T.R.C.L., Moura, R.O., Lima, M.C.A., Junior, L.B.C., Almeida, S.M.V., 2019. Topoisomerase inhibition and albumin interaction studies of acridine thiosemicarbazone derivatives. Int. J. Biol. Macromol. 138, 582–589. https://doi.org/10.1016/j.ijbiomac.2019.07.097.

Silva, P.R., Oliveira, J.F., Silva, A.L., Queiroz, C.M., Feitosa, A.P.S., Duarte, D.M.F.A., Lima, M.D.C.A., 2020. Novel indol-3-yl-thiosemicarbazone derivatives: obtaining, evaluation of in vitro leishmanicidal activity and ultrastructural studies. Chem. Biol. Interact. 315, 108899 https://doi.org/10.1016/j.cbi.2019.108899.

Szymaszek, P., Fiedor, P., Chachaj-Brekiesz, A., Tyszka-Czochara, M., Świergosz, T., Ortyl, J., 2022. Molecular interactions of bovine serum albumin (BSA) with pyridine derivatives as candidates for non-covalent protein probes: a spectroscopic investigation. J. Mol. Liq. 347 (2022), 118262 https://doi.org/10.1016/j.molliq.2021.118262.

Tenório, R.P., Góes, A.J., Lima, J.G.D., Faria, A.R.D., Alves, A.J., Aquino, T.M.D., 2005. Tiossemicarbazonas: métodos de obtenção, aplicações sintéticas e importância biológica. Quim. Nova 28, 1030–1037. https://doi.org/10.1590/S0100-40422005000600018.

Upegui, Y., Gil, J.F., Quiñones, W., Torres, F., Escobar, G., Robledo, S.M., Echeverri, F., 2014. Preparation of rotenone derivatives and in vitro analysis of their antimalarial, antileishmanial and selective cytotoxic activities. Molecules 19 (11), 18911–18922. https://doi.org/10.3390/molecules191118911.

Verhaeghe, P., Azas, N., Hutter, S., Castera-Ducros, C., Laget, M., Dumètre, A., Vanelle, P., 2009. Synthesis and in vitro antiplasmodial evaluation of 4-anilino-2-trichloromethylquinazolines. Bioorg. Med. Chem. 17, 4313–4322. https://doi.org/10.1016/j.bmc.2009.05.022.

Volynets, G.P., Tukalo, M.A., Bdzhola, V.G., Derkach, N.M., Gumeniuk, M.I., Tarnavskiy, S.S., Yarmoluk, S.M., 2019. Benzaldehyde thiosemicarbazone derivatives against replicating and nonreplicating Mycobacterium tuberculosis. J. Antibiot. Res. 72 (4), 218–224. https://doi.org/10.1038/s41429-019-0140-9.

Wang, W., Gao, D., Zheng, Q., Zhao, X., Na, R., Wan, Q., Li, X., 2021. Interactions of isoorientin and its Semi-synthetic analogs with human serum albumin. Bioorg. Chem. 116, 105319 https://doi.org/10.1016/j.bioorg.2021.105319.

WHO, 2020. Malaria. WHO. https://www.who.int/malaria/en/. (Accessed 11 May 2022).

World Health Organization, 2018. Neglected tropical diseases, 2017, Avaliable online at: https://www. who. int/news-room/qa-detail/neglected-tropical-diseases. (Accessed 4 May 2021).

World Health Organization, 2022. Ending the Neglect to Attain the Sustainable Development Goals: One Health: Approach for Action against Neglected Tropical Diseases 2021-2030.

Yıldız, M., Bingul, M., Zorlu, Y., Saglam, M.F., Boga, M., Temel, M., Sengul, I.F., 2022. Dimethoxyindoles based thiosemicarbazones as multi-target agents; synthesis, crystal interactions, biological activity and molecular modeling. Bioorg. Chem. 120, 105647 https://doi.org/10.1016/j.bioorg.2022.105647.

Zuma, A.A., Macedo-Silva, S.T., Achari, A., Vinayagam, J., Bhattacharjee, P., Chatterjee, S., et al., 2021. Furan derivatives impair proliferation and affect ultrastructural organization of Trypanosoma cruzi and Leishmania amazonensis. Exp. Parasitol. 224, 108100 https://doi.org/10.1016/j.exppara.2021.108100.